*proceedings*

MDPI

*Proceedings*

# Experimental Connection between the Instrumental and Bell Inequalities †

**Iris Agresti [1,*], Gonzalo Carvacho [1], Davide Poderini [1], Leandro Aolita [2,3], Rafael Chaves [4,5] and Fabio Sciarrino [1]**

1 Dipartimento di Fisica, Sapienza Università di Roma, Piazzale Aldo Moro 5, I-00185 Roma, Italy
2 Instituto de Física, Universidade Federal do Rio de Janeiro, Caixa Postal 68528, Rio de Janeiro 21941-972, Brazil
3 ICTP South American Institute for Fundamental Research, Instituto de Física Teórica, UNESP-Universidade Estadual Paulista, R. Dr. Bento T. Ferraz 271, Bl. II, São Paulo 01140-070, Brazil
4 International Institute of Physics, Federal University of Rio Grande do Norte, P. O. Box 1613, Natal 59078-970, Brazil
5 School of Science and Technology, Federal University of Rio Grande do Norte, Natal 59078-970, Brazil
* Correspondence: iris.agresti@uniroma1.it
† Presented at the 11th Italian Quantum Information Science conference (IQIS2018), Catania, Italy, 17–20 September 2018.

Received: 16 November 2018; Accepted: 30 December 2018; Published: 18 July 2019


**Abstract:** An investigated process can be studied in terms of the causal relations among the involved variables, representing it as a causal model. Some causal models are particularly relevant, since they can be tested through mathematical constraints between the joint probability distributions of the observables. This is a valuable tool because, if some data violates the constraints of a causal model, the implication is that the observed statistics is not compatible with that causal structure. Strikingly, when non-classical correlations come to play, a discrepancy between classical and quantum causal predictions can arise, producing a quantum violation of the classical causal constraints. The simplest scenario admitting such quantum violation is given by the instrumental causal processes. Here, we experimentally violate an instrumental test on a photonic platform and show how the quantum correlations violating the CHSH inequality can be mapped into correlations violating an instrumental test, despite the different forms of non-locality they display. Indeed, starting from a Bell-like scenario, we recover the violation of the instrumental scenario through a map between the two behaviours, which includes a post-selection of data and then we test an alternative way to violate the CHSH inequality, adopting the instrumental process platform.

**Keywords:** quantum information; quantum causality; causal inference; quantum violation; instrumental process; instrumental inequalities; chsh inequality

## 1. Introduction

A most relevant quest in science is inferring the causal relations underlying a system of interest, exploiting the statistics of collected data. To achieve this task, data needs to be supplemented with some causal assumptions, in order to falsify or validate a given causal model, taken as hypothesis [1]. A causal model is the representation of a process in terms of the causal relations among the involved variables, both those that are observables and those that are not (*latent* or *hidden*). All of the variables form a Bayesian network. The field that aims to determine whether observed data is compatible with a given Bayesian network or not is causal inference, largely studied by Pearl [2], and it relies on the mathematical constraints among the joint distributions of the observables. Indeed, some causal

models allow for inequalities, in the simplest cases made of linear combinations of the observed joint probabilities, which, if violated by data, lead to refute them as the causal structure underlying the system of interest. Unfortunately, this is not always the case, since not all causal models have testable implications.

For instance, the causal model represented in Figure 1a is compatible with any joint distribution of A and B and, if one wants to determine whether an event A affects or not an event B, observational data is not enough, one has to resort to interventions [2]. In turn, the causal models in Figure 1b,c have testable constraints already at the level of observational data. Hence, the simplest model, in terms of the number of nodes within the corresponding Directed Acyclic Graph (DAG) [2], to which we must resort to exclude that a variable A is affecting a variable B is the instrumental process (see Figure 1c), that admits the instrumental inequalities [1,3,4]. This makes the instrumental causal model an essential tool in a wide range of fields, from economics to medicine, as it allows to estimate causal dependencies even in the presence of unobserved common causes.

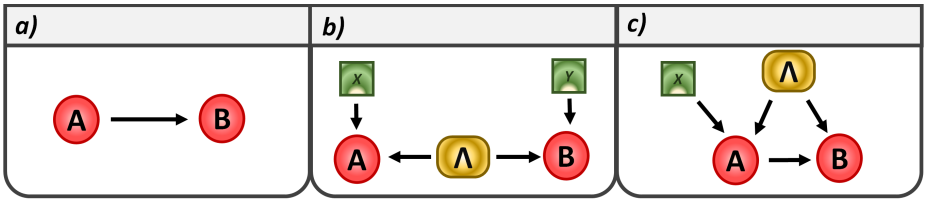


**Figure 1. Directed Acyclic Graphs representing causal models.** In this figure, we show three different causal models represented by Directed Acyclic Graphs (DAG) [2], where each node represents a variable and the arrows link variables between whom there is a causal relationship. (**a**) This is the simplest causal model in which a variable A has an influence over B, but it has no testable mathematical constraints characterizing the allowed joint probabilities $p(a,b)$. (**b**) The causal model of a CHSH scenario, where the parties Alice (A) and Bob (B) share a system and choose the basis on which to measure it according two independent variables, X and Y. Hence, no communication must occur between A and B. (**c**) DAG representing the instrumental scenario, whose main difference from the CHSH Bell-like scenario, is the presence of a classical channel of communication between the parties, i.e., A has a causal influence over B.

Strikingly, the mathematical constraints corresponding to a generic causal model do not necessarily hold, when switching from the classical to the quantum realm and this discrepancy between classical and quantum causal predictions have brought to the development of the field of quantum causal modelling [5–13]. The best known example is represented by the CHSH Bell inequality (see Figure 1b) [14,15]. This scenario is made of two parties, Alice and Bob, sharing a bipartite state, with the possibility to independently choose between two binary observables each (respectively A or A' and B or B'). In this context, if all the involved variables are classical, the following inequality holds: $S = |\langle A,B\rangle + \langle A,B'\rangle + \langle A',B\rangle - \langle A',B'\rangle| \leq 2$, where $\langle A,B\rangle = \sum_{a,b}(-1)^{a+b}p(a,b)$ and the sum is carried over the four combinations of Alice's and Bob's outputs $(a,b)$. When Alice and Bob share an entangled state, however, for dichotomic measurements, the upper bound of S shifts to $2\sqrt{2}$ (Tsirel'son bound) [16]. The same happens for many other causal structures, beyond the CHSH scenario, as investigated in many recent studies [17–23], and for some classes of non-trivial inequalities within instrumental scenario [3,4], where Bob's choice between $d$ binary observables is determined by the output of Alice's $d-outcome$ measurement while, in turn, Alice chooses among her $n$ observables, according to the value of a classical variable X, called *Instrument* [24]. Hence, the main difference between Bell-like and instrumental scenarios is constituted by the presence of a classical channel of communication between Alice and Bob.

In this work, we are showing the experimental violation of the following instrumental inequality on a photonic platform, reported for the first time in [24]: $\mathcal{I}_{322} = -\langle B\rangle_1 + 2\langle B\rangle_2 + \langle A\rangle_1 - \langle AB\rangle_1 + 2\langle AB\rangle_3 \leq 3$, where $\langle AB\rangle_x = \sum_{a,b}(-1)^{a+b}p(a,b|x)$ and the subscripts in $\mathcal{I}_{|x|,|a|,|b|}$ indicates the number

of possible values of the variables, $x$, $a$ and $b$. The upper limit of this inequality becomes $1+\sqrt{2} \approx 3.828$, when the parties share an entangled state. Then, we experimentally apply the theoretical results reported in [25], mapping the quantum correlations within the CHSH scenario into those of the instrumental. Indeed, it is possible to recover the instrumental inequality [3], expressing it as a function of the CHSH violation, obtained within a Bell-like scenario. This mapping, as mentioned before, requires a post-selection of the data collected in the Bell-like scenario, in order to simulate the communication channel between the parties characterizing the instrumental causal structure. Moreover, adopting the instrumental scenario, there is an alternative procedure, described in [25], to test the CHSH inequality, without the need of observing all the correlations for the 4 input pairs $(x,y) \in \{(0,0),(0,1),(1,0),(1,1)\}$.

## 2. Results

### *2.1. Active Feed-Forward of Information*

In order to experimentally implement an instrumental process and violate the aforementioned $\mathcal{I}_{322}$ inequality's upper bound, we adopt a photonic platform, depicted in Figure 2, encoding the qubits in the degree of freedom of the photons' polarization. The generated state is a singlet, $|\psi^-\rangle = \frac{|01\rangle - |10\rangle}{\sqrt{2}}$ obtained through a Spontaneous Parametric Down-Conversion process (which constitutes our hidden variable $\Lambda$).

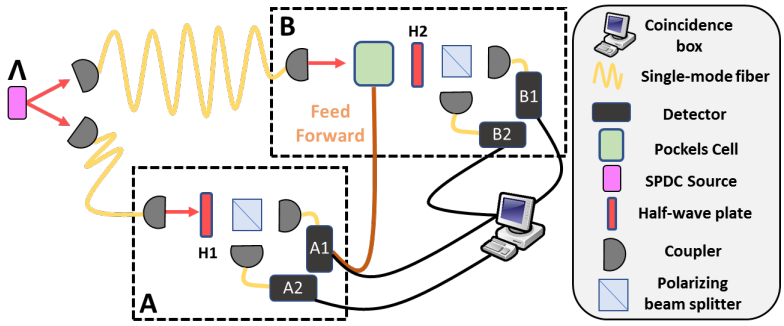


**Figure 2. Experimental Apparatus.** We generate a singlet state through a SPDC process (constituting our hidden variable $\Lambda$) that is shared by the two parties A and B. On A's path, the measurement station is made by a HWP followed by a PBS, since the qubits are encoded in the polarization of the photons. On B's path, there is an analogous measurement station, but, before the HWP $H_2$, we put a Pockels cell, to switch from one operator to the other, in the case of active feed-forward, i.e., triggering a high voltage application to the Pockels cell and making it behave as a HWP, while, when it is not triggered, it performs the identity. The voltage application is triggered by Alice's detector $A_1$ (i.e., corresponding to output 0), whose signal is split and sent both to a coincidence counter and to the Pockels cell. In the post-selection case, the Pockels cell is not triggered and A and B choose independently the measurement basis, performing the desired observables rotating respectively $H_1$ and $H_2$.

The pair of entangled photons is shared between Alice (A) and Bob (B). The two parties' measurement stations are composed by a half-wave plate (HWP) followed by a Polarizing Beam Splitter (PBS). The communication channel is implemented putting a Pockels cell on Bob's path, before the HWP $H_2$, connected to Alice's detector $A_1$. Hence, when this detector clicks (corresponding to Alice's outcome 0), its signal is split and sent both to the Pockels cell and to a coincidence counter. The signal triggers the application of a high voltage ($\sim$1250 V) to the cell, which then behaves like a HWP, while otherwise it performs the identity. In this way, we can switch between the two observables on Bob's side, within the order of nanoseconds time. In the meantime, Bob's photon is delayed through a 125 m long single-mode fiber, which delays the photon of $\sim$600 ns. We refer to this kind of communication channel between A and B as *active feed-forward of information* [26,27].

In the present case, where the generated state is $|\psi^-\rangle$, we make Alice choose the observables to perform among $(\sigma_x - \sigma_z)/\sqrt{2}$, $-\sigma_x$ and $\sigma_z$ and Bob between $(\sigma_x - \sigma_z)/\sqrt{2}$ and $-(\sigma_x + \sigma_z)/\sqrt{2}$. The observed violation of $\mathcal{I}_{322} \leq 3$ instrumental inequality is $\mathcal{I}_{322} = 3.358 \pm 0.020$.

### 2.2. Post-Selection Scenario

The aforementioned classical channel of communication between the parties characterizing the instrumental process, experimentally implemented through the trigger of the Pockels cell, can be also simulated through a post-selection of data. In other words, through the same experimental apparatus (see Figure 2), we keep the Pockels cell switched off and perform, through the rotation of $H_1$ and $H_2$ HWP, all the combinations of Alice's and Bob's observables. Afterwards, we take into account only the events for which Bob's choice corresponds to Alice's outcome. We apply this procedure to violate Bonet's instrumental inequality [3], i.e., $\mathcal{I}_{Bonet} = p(a = b|0) + p(b = 0|1) + p(a = 0, b = 1|2) \leq 2$ where the involved probabilities are expressed as $p(a, b|x)$. In this case, when Alice and Bob share a bipartite entangled state, $\mathcal{I}_{Bonet}$'s value can be larger than 2, up to $(3 + \sqrt{2})/2 \approx 2.207$, and the maximal violation corresponds to 2-qubit maximally entangled states, as before. The observables that correspond to the maximal violation, for the quantum state $|\psi^-\rangle$, are $-\sigma_x$, $\sigma_z$ and $(\sigma_x - \sigma_z)/\sqrt{2}$ for Alice and $(\sigma_x - \sigma_z)/\sqrt{2}$ and $(\sigma_x + \sigma_z)/\sqrt{2}$ for Bob, respectively when he gets $a = 0, 1$ as input. The obtained violations are reported in purple in Figure 3, whose weighted average is: $2.1713 \pm 0.0022$.

The most interesting feature of this procedure is that, since there is no active feed-forward of information, Alice and Bob choose their measurements bases independently, as in a Bell-like test. As a matter of fact, in [24] it has been shown that performed in this way the instrumental scenario can be seen as testing a stronger form of non-classicality, showing the incompatibility of quantum correlations with specific classes of non-local hidden variable models. However, if we indicate respectively with $n$ and $d$ the number of observables among which Alice and Bob can choose, a quantum violation of the instrumental scenario cannot be observed for $(n, d) < (3, 2)$ [9,24], while, for the case $(n, d) = (2, 2)$, the CHSH inequality can be violated. Anyway, as we show experimentally in what follows, any quantum correlations in the CHSH scenario can be used as a resource to violate Bonet's inequality.

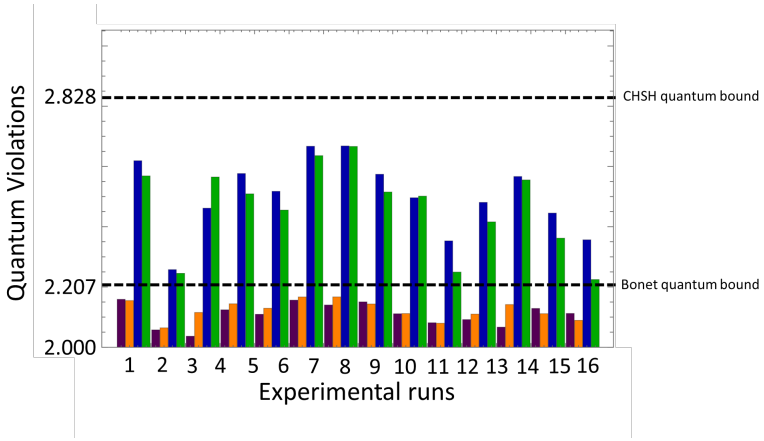


**Figure 3. Experimental results.** In this plot we show the experimental quantum violations of Bonet and CHSH inequalities obtained from 16 experimental runs in the post-selection regime (for both scenarios the classical upper bound is 2). In purple and blue, we show respectively the Bonet's and CHSH violations obtained through the apparatus described in Figure 2 section, keeping the Pockels cell switched off and performing Alice's and Bob's measurements, rotating the HWPs. In orange, we show the extent of the Bonet inequality's violation that can be obtained from the probabilities p(a,b | x,y) belonging to the CHSH scenario. In green, we show the CHSH violation obtained on an instrumental process platform, through an alternative procedure which does not require the correlations between all of the 4 combinations of the inputs (x,y).

#### 2.2.1. Relation between Bonet and CHSH Inequality Violation

Adopting the apparatus depicted in Figure 2, with no active feed-forward, we make Alice and Bob independently choose respectively the observables to apply to $|\psi^-\rangle$ between $-\sigma_x$ and $\sigma_z$ and between $(\sigma_x - \sigma_z)/\sqrt{2}$ and $(\sigma_x + \sigma_z)/\sqrt{2}$ (we are in the regime $n = 2, d = 2$). Then, we combine the observed mean values, to evaluate the corresponding S. The obtained violations of the CHSH inequality are represented in blue, in Figure 3, whose weighted average is: $2.5518 \pm 0.0020$.

Now, from these CHSH violations, we want to violate Bonet's instrumental inequality. Hence, in order to express $\mathcal{I}_{Bonet}$ as a function of the probability distributions obtained within the Bell scenario, we need to lift Bonet's inequality via the mapping $p(a, b|x) \to p(a, b|x, y = a)$. We therefore find $\mathcal{I}^{lifted}_{Bonet} = \frac{1}{4}\langle CHSH\rangle - p(11|20) + \frac{3}{2}$ [25]. To evaluate $p(11|20)$, we must map the $p(a, b|x, y)$ characterizing the CHSH scenario, which belongs to the case ($n = 2, d = 2$), to $p'(a, b|x, y)$, with ($n = 3$, $d = 2$). This map is $p'(a, b|x, y) = p(a, b|x, y)$ for $x = 0, 1$ and $p'(a, b|2, y) = \delta_{a,0}p(b|y)$ for $x = 2$, making $p'(11|20) = 0$.

So the relation between $\mathcal{I}_{Bonet}$ and the CHSH inequality, for $p'(a, b|x, y)$, is $I^{p'}_{Bonet} = \frac{1}{4}\langle CHSH\rangle + \frac{3}{2}$. It is noteworthy to stress that the existence of this mapping does not imply that the non-classicality revealed by the violation of a Bell inequality or an instrumental are of the same kind. Indeed, the data post-selection, which is required by this procedure, is not a Bell non-locality free operation, as it can increase the non-locality of the observed behaviour. The need of performing a post-selection to move from one scenario to the other already suggests that the non-classicality of the correlations revealed by a quantum violation of the instrumental inequalities is stronger than in a Bell-like scenario (see [24] for further details).

The obtained Bonet's inequality violations are represented in orange in Figure 3, whose weighted average is: $2.10218 \pm 0.00089$.

#### 2.2.2. CHSH Violation within an Instrumental Process

The connection between the instrumental and the CHSH scenario can also be expressed as follows: $\frac{1}{4}\langle CHSH\rangle_p + \frac{3}{2} = p(00|00) + p(11|01) + p(00|10) + p(10|11) + p_{B|Y}(1|0)$. Hence, the CHSH can be alternatively tested using 3 choices of an input $X$, instead of testing the correlations between the 4 choices of the inputs $(x, y)$. In this procedure, when $x = 0, 1$ Alice's output selects Bob's choice, as in the usual instrumental scenario, while, when $x = 2$, Alice's party is not tested, while Bob's input is deterministically equal to 0 and his output is registered, in order to evaluate $p_{B|Y}(1|0)$. Through this procedure, we obtained the CHSH violation represented in green in Figure 3, whose weighted average is: $2.5053 \pm 0.0039$.

## 3. Discussion

Summarizing, in this work, we experimentally study the instrumental scenario, showing the violation of an equivalent of Bonet's inequality (indicated in the text as $\mathcal{I}_{322}$) on a photonic platform. Then, we apply the theoretical results of [25] and experimentally confirm that the non-classical correlations revealed by a CHSH quantum violation, augmented by a non-local post-selection operation whereby Bob's input is set equal to Alice's output, give rise to the quantum violation of Bonet's instrumental inequality. We note that, in [25], it is claimed that since, upon such behaviour mapping, Bonet's inequality is violated if and only if the CHSH inequality is violated, both these violations witness one and the same form of non-locality. However, as mentioned before, the mapping relies on a non-local post-selection of data, which is a highly resourceful operation from the point of view of non-locality. Therefore, although the connection between instrumental and Bell violations is undoubtedly notorious, we believe it is fair to say that correlations violating instrumental inequalities display an intrinsically different (and, in a sense, stronger) form of non-locality than those violating Bell inequalities. Indeed the latter must be enhanced with non-local post-selections to reach the former. In short, when viewed from a Bell's scenario perspective, the violation of the instrumental inequality

without active feed-forward of information is testing the incompatibility of quantum correlations with a specific class of non-local hidden variable models (that include local models as a particular case), thus clearly testing for a stronger form of non-locality. As for the experiment, adopting the collected data of a CHSH scenario, we were able to obtain the violation extent of Bonet's inequality and test the CHSH inequality from the data collected within an instrumental process (i.e., with Alice affecting Bob's operator choice). The interest in the study of the instrumental scenario and its relation to Bell-like tests originates from the possible application of this newly investigated quantum causal tool for quantum information processing tasks, for example in cryptographic protocols or randomness generation.

## 4. Materials and Methods

Photon pairs were generated in a parametric down conversion source, composed by a nonlinear crystal Beta-Barium Borate (BBO) of 2 mm-thick injected by a pulsed pump field with $\lambda = 392.5$ nm. After spectral filtering and walk-off compensation, photons of $\lambda = 785$ nm are sent to the two measurement stations A and B. The crystal used to implement active feed-forward is a LiNbO3 high-voltage micro Pockels Cell made by Shangai Institute of Ceramics with <1 ns risetime and a fast electronic circuit transforming each Si-avalanche photodetection signal into a calibrated fast pulse in the kV range needed to activate the Pockels Cell is fully described in [26,27]. To achieve the active feed-forward of information, the photon sent to Bob's station needs to be delayed, thus allowing the measurement on the first qubit to be performed. The amount of delay was evaluated considering the velocity of the signal transmission through a single mode fiber and the activation time of the Pockels cell.

**Acknowledgments:** LA acknowledges financial support from the Brazilian agencies CNPq (PQ grant No. 311416/2015-2 and INCT-IQ), FAPERJ (JCNE), CAPES, and FAPESP, and the Serrapilheira Institute (grant number Serra-1709-17173). RC acknowledges financial support from the Brazilian ministries MEC and MCTIC, funding agency CNPq (PQ grant No. 307172/2017-1 and INCT-IQ) and the Serrapilheira Institute (grant number Serra-1708-15763). G. C. thanks Becas Chile and Conicyt. We acknowledge support from John Templeton Foundation via the grant Q-CAUSAL n°61084 (the opinions expressed in this publication are those of the authors and do not necessarily reflect the views of the John Templeton Foundation)

**Conflicts of Interest:** The authors declare no conflict of interest.

## Abbreviations

The following abbreviations are used in this manuscript:

| | |
|---|---|
| CHSH | Clauser-Horne-Shimony-Holt inequality |
| DAG | Directed Acyclic Graph |
| HWP | Half-wave plate |
| PBS | Polarizing Beam Splitter |
| BBO | Beta-Barium Borate |
| SPDC | Spontaneous Parametric Down-Conversion |

## References

1. Pearl, J. On the testability of causal models with latent and instrumental variables. In Proceedings of the 11th conference on Uncertainty in artificial intelligence (UAI '95), Montreal, QC, Canada, 18–20 August 1995; pp. 435–443.
2. Pearl, J. *Causality: Models, Reasoning and Inference*, 2nd ed.; Cambridge University Press: New York, NY, USA, 2009; ISBN 978-0521895606.
3. Bonet, B. Instrumentality Tests Revisited. In Proceedings 17th Conference Uncertainty in Artificial Intelligence, Seattle, WA, USA, 2–5 August 2001; pp. 48–55.
4. Popescu, S.; Rohrlich, D. Quantum Nonlocality as an axiom. *Found. Phys.* **1994**, *24*, 379-385.
5. Leifer, M.S.; Spekkens, R.W. Towards a formu- lation of quantum theory as a causally neutral theory of bayesian inference. *Phys. Rev. A* **2013**, *88*, 052130.

6. Fritz, T. Beyond bell's theorem ii: Scenarios with arbitrary causal structure. *Commun. Math. Phys.* **2016**, 341, 391–434.
7. Procopio, L.M.; Moqanaki, A.; Araújo, M.; Costa, F.; Calafell, I.A.; Dowd, E.G.; Hamel, D.R.; Rozema, L.A.; Brukner, C.; Walther, P. Experimental superposition of orders of quantum gates. *Nat. Comm.* **2015**, *6*, 7913.
8. Rubino, G.; Rozema, L.A.; Feix, A.; Araújo, M.; Uner, J.M.Ze.; Procopio, L.M.; Brukner, C.; Walther, P. Experimental verification of an indefinite causal order. *Sci. Adv.* **2017**, *3*, e1602589.
9. Henson, J.; Lal, R.; Pusey, M.F. Theory-independent limits on correlations from generalized bayesian networks. *New J. Phys.* **2014**, *16*, 113043.
10. Chaves, R.; Majenz, C.; Gross, D. Information-theoretic implications of quantum causal structures. *Nat. Commun.* **2015**, *6*, 5766.
11. Costa, F.; Shrapnel, S. Quantum causal modelling. *New J. Phys.* **2016**, *18*, 063032.
12. Allen, J.-M.A.; Barrett, J.; Horsman, D.C.; Lee, C.M.; Spekkens, R.W. Quantum common causes and quantum causal models. *Phys. Rev. X* **2016**, *7*, 031021.
13. Pienaar, J.; Brukner, C. A graph-separation theorem for quantum causal models. *New J. Physics* **2015**, *17*, 073020.
14. Bell, J. On the Einstein Podolsky Rosen paradox. *Phys. Phys. Fizika* **1964**, *1*, 195–200.
15. Clauser, J.F.; Horne, M.A.; Shimony, A.; Holt, R.A. Proposed experiment to test local hidden-variable theories. *Phys. Rev. Lett.* **1969**, *23*, 880–884, .
16. Cirel'son, B.S. Quantum generalizations of Bell's inequality. *Lett. Math. Phys.* **1980**, *4*, 83.
17. Carvacho, G.; Andreoli, F.; Santodonato, L.; Bentivegna, M.; Chaves, R.; Sciarrino, F. Experimental violation of local causality in a quantum network. *Nat. Comm.* **2017**, *8*, 14775.
18. Andreoli, F.; Carvacho, G.; Santodonato, L.; Bentivegna, M.; Chaves, R.; Sciarrino, F. Experimental bilocality violation without shared reference frames. *Phys. Rev. A* **2015**, *95*, 062315.
19. Saunders, D.J.; Bennet, A.J.; Branciard, C.; Pryde, G.J. Experimental demonstration of nonbilocal quantum correlations. *Sci. Adv.* **2017**, *3*, e1602743.
20. Ringbauer, M.; Chaves, R. Probing the non- classicality of temporal correlation.*Quantum* **2017**, *1*, 35.
21. Ringbauer, M.; Giarmatzi, C.; Chaves, R.; Costa, F.; White, A.G.; Fedrizzi, A. Experimental test of nonlocal causality. *Sci. Adv.* **2016**, *2*, e1600162.
22. Chaves, R. Polynomial bell inequalities. *Phys. Rev. Lett.* **2016**, *116*, 010402.
23. Lee, C.M.; Horan, M.J. Towards Device-Independent Information Processing on General Quantum Networks. *Phys. Rev. Lett.* **2018**, *120*, 020504.
24. Chaves, R.; Carvacho, G.; Agresti, I.; di Giulio, V.; Aolita, L.; Giacomini, S.; Sciarrino, F. Quantum violation of an instrumental test. *Nat. Phys.* **2018**, *14*, 291–296.
25. Van Himbeeck, T.; Brask, J.B.; Pironio, S.; Ramanathan, R.; Sainz, A.B.; Wolfe, E. Quantum violations in the instrumental scenario and their relations to the Bell scenario. *arXiv* **2018**, arXiv:1804.04119.
26. Sciarrino, F.; Ricci, M.; de Martini, F.; Filip, R.; Mista, L. Realization of a minimal disturbance quantum measurement. *Phys. Rev. Lett.* **2006** , *96*, 020408, .
27. Giacomini, S.; Sciarrino, F.; Lombardi, E.; de Martini, F. Active teleportation of a quantum bit. *Phys. Rev. A* **2002**, *66*, 030302.